

Determination of Σ - Λ Relative Parity*

CYNTHIA ALFF,† N. GELFAND, U. NAUENBERG,‡ M. NUSSBAUM,
J. SCHULTZ,§ AND J. STEINBERGER
Columbia University, New York, New York

H. BRUGGER, L. KIRSCH, AND R. PLANO
Rutgers, The State University, New Brunswick, New Jersey^{||}

D. BERLEY AND A. PRODELL
Brookhaven National Laboratory, Upton, New York

(Received 15 September 1964)

An experiment has been performed to determine the Σ - Λ relative parity, through a study of the decay mode $\Sigma^0 \rightarrow \Lambda^0 + e^+ + e^-$. The Σ^0 were produced by stopping K^- mesons in the Brookhaven National Laboratory-Columbia 30-in. hydrogen chamber, in the reaction $K^- + p \rightarrow \Sigma^0 + \pi^0$, and 314 events were identified. The experimental distribution of the combined mass of the electron-positron pair was compared to that predicted by Feinberg, by Feldman and Fulton, and by Evans. If it is assumed that the dependence of the form factors on the combined mass of the electron-positron pair can be neglected, and that the ratio of the electric form factor F_1 to the magnetic form factor F_2 is less than 6, then the data show that the Σ - Λ relative parity is even.

I. INTRODUCTION

THE relative parities of the strange particles and, in particular, the Λ^0 and Σ^0 hyperons are of interest because of the symmetry requirements of various classification schemes proposed for elementary particles. For example in the "eightfold way" scheme proposed by Gell-Mann¹ the Λ^0 singlet and the Σ - Σ^0 ⁺ triplet are closely related. The Λ^0 and Σ^0 are viewed as different linear combinations of the same two fundamental baryon states, and the relative parity is required to be even. Other models, such as that of Barshay and Schwartz,² which pictures the Σ as a bound π - Λ s state, or that of Nambu and Sakurai,³ which suggests a strong $\pi\Lambda\Sigma$ scalar coupling, require that the Σ - Λ relative parity be odd. A measurement of the Σ - Λ relative parity would thus eliminate some theories and lend support to others.

The measurement of the relative parities of the strange particles is made difficult by the nonconservation of parity in the weak interactions, through which many of the strange particles decay. The measurement of the relative parities must proceed through investigation of the strong and electromagnetic interactions, both of which conserve strangeness. This makes a determination of the "absolute" parity with respect to the nucleons impossible for particles of strangeness 1; only the relative parities of such particles are measurable.

* Research supported in part by U. S. Atomic Energy Commission.

† Submitted in partial fulfillment of the requirements for the degree of Doctor of Philosophy in the Faculty of Pure Science, Columbia University.

‡ Present address: Princeton University, Princeton, New Jersey.

§ Present address: University of California, Berkeley, California.

^{||} Research supported in part by National Science Foundation.

¹ M. Gell-Mann, CTSL Report No. 20 1961 (unpublished); Phys. Rev. **125**, 1067 (1962).

² S. Barshay and M. Schwartz, Phys. Rev. Letters **4**, 618 (1960).

³ Y. Nambu and J. J. Sakurai, Phys. Rev. Letters **6**, 377 (1961).

The Σ - Λ relative parity may be obtained both directly, by investigation of reactions involving both Σ and Λ particles, and indirectly, by measuring the K - Λ and K - Σ relative parities. We shall review the existing evidence briefly.

A. K - Λ Parity

The K - Λ parity may be inferred to be odd from the existence of the reaction $K^- + \text{He}^4 \rightarrow \Lambda \text{He}^4 + \pi^-$, as argued by Dalitz.⁴ This reaction has been observed by Leitner *et al.*⁵ Assuming that all the particles in the reaction have 0 spin, there is no change in orbital angular momentum, and the (relative K - Λ parity) = (relative Λ -nucleon parity)(π -parity). Therefore, since the Λ -nucleon parity is defined to be even, the K - Λ relative parity is odd. To justify the assumption that the spin of the hyperfragment ΛHe^4 is 0, Dalitz considers ΛH^4 , the other member of the isospin doublet. The spin of the ΛHe^4 hyperfragment is the same as the spin of ΛH^4 by charge symmetry. The spin of ΛH^4 may be inferred from a study of the spin dependence of the branching ratio R_4 . R_4 is the fraction of mesonic decay of ΛH^4 in the mode $\Lambda \text{H}^4 \rightarrow \pi^- + \text{He}^4$. Dalitz and Liu⁶ have calculated R_4 as a function of the spin of ΛH^4 and of the ratio $P^2/(P^2+S^2)$, where P and S are the P and S wave amplitudes of the decay $\Lambda \rightarrow p + \pi$. The experimental limit⁷ on R_4 and on the ratio $P^2/(P^2+S^2)$ are only consistent with spin $\Lambda \text{H}^4 = 1$ for high values of $P^2/(P^2+S^2)$. In the view of Karplus and Ruderman⁸ such a high value of the ratio would lead to a rate for nonmesonic decays which is higher than that seen, and thus the ΛH^4 spin is believed to be 0.

⁴ R. H. Dalitz and B. W. Downs, Phys. Rev. **111**, 967 (1958).

⁵ J. Leitner, L. Gray, E. Harth, S. Lichtman, J. Westgard *et al.*, Phys. Rev. Letters **7**, 264 (1961).

⁶ R. H. Dalitz and L. Liu, Phys. Rev. **116**, 1312 (1959).

⁷ R. G. Ammar, R. Levi Setti, W. E. Slater, S. Limentani, P. E. Schlein, and P. H. Steinberg, Nuovo Cimento **19**, 20 (1961).

⁸ M. Ruderman and R. Karplus, Phys. Rev. **102**, 247 (1956).

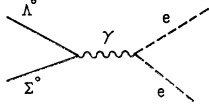


FIG. 1. Feynman diagram for the decay $\Sigma^0 \rightarrow \Lambda^0 + e^+ + e^-$.

In the light of recent evidence⁹ that the $K^- + \text{He}^4$ capture may be from a P state, it should be emphasized that the above argument is independent of the orbital angular momentum in the capture process. If, on the other hand, the ${}_{\Lambda}\text{He}^4$ spin were 1, and the capture from an S state, then the parity would be even. If the ${}_{\Lambda}\text{He}^4$ spin were 1, and the capture from a P state, then the K - Λ relative parity could not be determined from the reaction $K^- + \text{He}^4 \rightarrow {}_{\Lambda}\text{He}^4 + \pi^-$.

B. K - Σ Parity

The relative K - Σ parity has been studied by Tripp, Watson, and Ferro-Luzzi,¹⁰ who have measured the reaction $K^- + p \rightarrow Y^*$ (1520 MeV, $J = \frac{3}{2}$, $I = 0$, parity even with respect to K - p)

$$\begin{aligned} Y^* &\rightarrow \Sigma^+ + \pi^-, \\ Y^* &\rightarrow \Sigma^- + \pi^+, \\ Y^* &\rightarrow \Sigma^0 + \pi^0. \end{aligned}$$

The angular momentum of the initial state has been argued¹¹ to be S and D with some P_1 , so that by measuring the angular distribution and polarization of the Σ hyperons, the parity can be argued. The phases and amplitudes of the wave function are derived from the Σ^+ , Σ^- , and Σ^0 cross sections below the resonance threshold. Since there are three Σ cross sections, the isospin 1, S -wave amplitude, the isospin 0, S -wave amplitude and their phases may be found. The amplitude and relative phase of the isospin 0, D wave resonance are derived from the partial decay rates

$$\begin{aligned} Y^* &\rightarrow KN, \\ Y^* &\rightarrow \Sigma\pi, \\ Y^* &\rightarrow \Lambda\pi\pi. \end{aligned}$$

The relative S - D phase may be obtained by fitting the S - D interference terms in the angular distribution to the data. On the basis of the rather complicated analysis it is argued that the K - Σ parity is odd. Combined with the result of Leitner *et al.*,⁸ that the K - Λ parity is odd, this implies even Σ - Λ parity.

We report here an experiment to determine the Σ^0 - Λ^0 parity directly, following a suggestion of Feinberg,¹² that the decay $\Sigma^0 \rightarrow \Lambda^0 + e^+ + e^-$ differs in a predictable way of the two possible relative parities of the Σ^0 and Λ^0 .

II. THEORETICAL PREDICTION

The distribution in the decay $\Sigma^0 \rightarrow \Lambda^0 + e^+ + e^-$ has been calculated¹²⁻¹⁴ by considering the diagram of Fig. 1, in perturbation theory. On the basis of invariance arguments, the current at the Σ - Λ vertex must have the form³

$$J_{\mu} = e \left[\left(i\gamma_{\mu} \frac{k^2}{M^2} + \frac{\Delta}{M^2} k_{\mu} \right) F_1 + i\sigma_{\mu\nu} \frac{k_{\nu}}{M} F_2 \right]$$

in the case of even parity,

$$= e\gamma_5 \left[\left(i\gamma_{\mu} \frac{k^2}{M^2} + \frac{2k_{\mu}}{M} \right) F_1 + i\sigma_{\mu\nu} \frac{k_{\nu}}{M} F_2 \right]$$

in the case of odd parity,

where $\Delta = \Sigma$ - Λ mass difference and $M =$ average of the Σ - Λ masses.

The transition probability may be written in terms of the variables x and y introduced by Kroll and Wada¹⁵ where

$$x = [(E_+ + E_-)^2 - (\mathbf{P}_+ + \mathbf{P}_-)^2]^{1/2},$$

$$y = \frac{E_- - E_+}{|\mathbf{P}_- + \mathbf{P}_+|}.$$

E_- , E_+ , \mathbf{P}_- , and \mathbf{P}_+ are the energies and momenta of the electron and positron. The theoretical spectra are

$$\begin{aligned} \frac{d^2\rho_{\pm}(x,y)}{dx dy} &= \frac{\alpha}{4\pi} \left(\frac{M_{\Sigma}}{\Delta} \right)^3 \frac{1}{M_{\Sigma} M} \frac{q}{x^3} \\ &\times \left\{ \frac{|F_2(x)|^2}{|F_2(0)|^2} \frac{1}{M^2} [(x^2 + 2m^2)(2M_{\Sigma}q^2 + q_0^2x^2 \mp M_{\Lambda}x^2) - M_{\Sigma}q^2x^2(1-y^2)] + \frac{2 \operatorname{Re}F_1(x)F_2^*(x)}{F_2(0)^2} \frac{x^2}{M^3} (2m^2 + x^2) \right. \\ &\left. \times [x^2 - (M_{\Sigma} - q_0)(M_{\Sigma} \mp M_{\Lambda})] + \frac{|F_1(x)|^2}{|F_2(0)|^2} \frac{x^4}{M^4} [(x^2 + 2m^2)(q_0 \mp m_{\Lambda}) + M_{\Sigma}q^2(1-y^2)] \right\}, \quad (1) \end{aligned}$$

⁹ J. G. Fetkovich and E. G. Pewitt, Phys. Rev. Letters **11**, 290 (1963); M. M. Block, T. Kikuchi, D. Koetke, J. Kopelman, C. R. Sun, R. Walker, G. Culligan, V. L. Telegdi, and R. Winston, *ibid.* **11**, 301, (1963).

¹⁰ R. D. Tripp, M. B. Watson, and M. Ferro-Luzzi, Phys. Rev. Letters **8**, 175 (1962).

¹¹ M. Ferro-Luzzi, R. D. Tripp, and M. B. Watson, Phys. Rev. Letters **8**, 28 (1962).

¹² G. Feinberg, Phys. Rev. **109**, 1019 (1958).

¹³ G. Feldman and T. Fulton, Nucl. Phys. **8**, 106 (1958).

¹⁴ I. E. Evans, Nuovo Cimento **25**, 580 (1962); University of Wisconsin report (unpublished).

¹⁵ N. M. Kroll and W. Wada, Phys. Rev. **98**, 1355 (1955).

where

$d^2\rho_+(x,y)/dxdy$ is the even parity spectrum; choose the upper sign,

$d^2\rho_-(x,y)/dxdy$ is the odd parity spectrum; choose the lower sign.

$M_\Sigma = \Sigma^0$ mass, $M_\Lambda = \Lambda^0$ mass, $m = e$ mass, $q =$ c.m. momentum of Λ^0 , and $q_0 =$ c.m. energy of $\Lambda^0 = (q^2 + m_\Lambda^2)^{1/2}$. The spectra are normalized to the $\Sigma^0 \rightarrow \Lambda^0 + \gamma$ transition probability. Let us call the term involving $|F_2(x)|^2 / |F_2(0)|^2$ the leading term. The terms multiplying F_1 and F_1^2 are smaller by a factor of roughly 10^3 and 10^6 , respectively, owing to the baryon mass term in the denominator.

We may obtain the distribution as a function of x or y separately by integrating over y or x , respectively. The results are

$$\frac{d\rho_\pm(x)}{dx} \equiv \int_{-(1-4m^2/x^2)^{1/2}}^{+(1-4m^2/x^2)^{1/2}} \frac{d^2\rho_\pm(x,y)}{dxdy} dy = \frac{\alpha}{2\pi} \left(\frac{M_\Sigma}{\Delta} \right)^3 \frac{q(1-4m^2/x^2)^{1/2}}{M_\Sigma M x^3} \times \left\{ \frac{F_2(x)^2}{F_2(0)^2} \frac{1}{M^2} [(x^2+2m^2)(\frac{2}{3}M_\Sigma q^2 + x^2(q_0 \mp M_\Lambda))] + 2 \operatorname{Re} \frac{F_1(x)F_2^*(x)}{|F_2(0)|^2} \frac{x^2}{M^3} (x^2+2m^2) \right. \\ \left. \times [\frac{|F_1(x)|^2}{F_2(0)^2} \frac{x^2}{M^4} (x^2+2m^2) [\frac{2}{3}M_\Sigma q^2 + x^2(q_0 \mp M_\Lambda)]] \right\}, \quad (2)$$

$$\frac{d\rho_\pm(y)}{dy} \equiv \int_{2m/(1-Y^2)^{1/2}}^{\Delta} \frac{d^2\rho_\pm(x,y)}{dxdy} dx = \frac{\alpha}{8\pi} \frac{M_\Lambda M_\Sigma}{M^2} \left\{ \frac{F_1^2}{F_2(0)^2} \frac{\Delta^2}{M^2} [(1+y^2)^{\frac{2}{3}} \delta^3 (1 - \frac{1}{5}(3\delta^2 - 1))] \right. \\ \left. + (2/15)\delta^3(3\delta^2 - 1)(1 \mp 1) - 2 \operatorname{Re} \frac{(F_1 F_2^*)}{F_2(0)^2} \frac{\Delta^2}{M M_\Lambda} \left(\frac{\frac{2}{3}\delta^3}{\Delta} \left[\frac{M_\Sigma \mp M_\Lambda}{\Delta} - \frac{1}{5}(3\delta - 1) \right] \right) \right. \\ \left. + \frac{|F_2|^2}{|F_2(0)|^2} \left((1+y^2) \left[\ln \frac{1+\delta}{1-\delta} - 2\delta - \frac{2}{3}\delta^3 \right] + \frac{2}{3}\delta^3(1 \mp 1) \right) \right\}, \quad (3)$$

where

$$\rho = \left(1 - \frac{4m^2}{\Delta^2(1-y^2)} \right)^{1/2}.$$

In the case of integration over x , we have assumed that the form factors are independent of x , and we have made the approximation

$$q_0 \cong M_\Lambda + \mathbf{q}^2/2M_\Lambda.$$

In order to use the relations (1), (2), and (3) in the discussion of the $\Sigma^0 - \Lambda^0$ relative parity, it is necessary to understand both the relative magnitudes of $F_1(x)$ and $F_2(x)$ on the one hand, and their dependence on x on the other.

Feinberg¹ has estimated the extent of their x dependence in the region $4m^2 < x^2 < \Delta^2$, by expanding the form factors in a power series in x^2 .

$$F(x^2) = F(0) + \frac{1}{6}R^2 x^2 \dots$$

R is considered to be an effective electromagnetic radius, due to strong interactions at the $\Sigma\Lambda\gamma$ vertex. If we consider $R \cong 1/m_\pi$ to be an upper limit on the radius, then we get for the fractional change in the form factor in the region of interest

$$\frac{F(x^2 = \Delta^2) - F(x^2 = 4m_e^2)}{F(0)} = \frac{-4m_e^2 + \Delta^2}{6m_\pi^2 F(0)} = 5\%$$

since $F(0) \sim 1$.

Evans³ has used dispersion theory to estimate the form factor dependence on x , in a manner similar to that of Frazer and Fulco¹⁶ in calculations of the nuclear form factors. The result of Evans is that

$$[F_2(x^2)]/[F_2(0)] \sim [F_2^V(x^2)]/[F_2^V(0)],$$

where F_2^V is the nuclear isovector form factor. This results in a variation of F_2 throughout the range of x of about 1.5%. The spectrum $d\rho_\pm(x)/dx$ is sufficiently sensitive to the $\Sigma - \Lambda$ relative parity so that changes of this order of magnitude would not affect the parity determination. In the analysis of our experimental distribution, we have taken the form factors F_1 and F_2 to be constants; $F_1(x) = F_1(0)$, $F_2(x) = F_2(0)$.

The question of the magnitude of F_1 is more obscure. F_1 would be zero for a neutral particle with no electromagnetic structure. The F_1 term is due to the "finite size" of the strongly interacting hyperon. Feldman and Fulton¹³ have performed a perturbation theory calculation and obtain the result

$$\operatorname{Re} \frac{(F_1 F_2^*)}{|F_2(0)|^2} = 0.25 \text{ for odd relative parity.}$$

¹⁶ W. R. Frazer and J. R. Fulco, Phys. Rev. Letters 2, 365 (1959); Phys. Rev. 117, 1603 and 1609 (1960).

The calculation is not rigorous and it is not possible to estimate the error in the result. However, Fulton¹⁷ points out that similar calculations¹⁸ in the case of the nucleon anomalous moments give values within a factor of 2 or 3 of the measured moments. If F_1 is of this order of magnitude, the contribution of F_1 in the case of either parity is too small to be measurable in this experiment. In the case of even parity, the F_1 terms remain negligible for any conceivable value of the ratio F_1/F_2 . In the odd parity case, the F_1 term becomes comparable to the F_2 term at large values of x if $F_1 \sim 8F_2$.

Assuming for the moment that $F_1/F_2 \ll 8$, we note that in that case, the spectrum in y (Form. 3) is similar for the two particles; however, the distribution in x (Form. 2) is substantially different for large values of x (see Figs. 5 and 6). This difference forms the basis of the parity determination attempted in this experiment.

III. EXPERIMENTAL PROCEDURES

A. Beam

With the foregoing considerations in mind, we have performed an experiment to study the decay $\Sigma^0 \rightarrow \Lambda^0 + e^+ + e^-$. The Σ^0 were produced in the 30-in. Brookhaven National Laboratory-Columbia Hydrogen Bubble Chamber in the reaction $K^- + p \rightarrow \Sigma^0 + \pi^0$ at rest. A separated beam was designed to transport the K^- mesons from the internal target in the AGS ring to the chamber. The K^- mesons were produced by the internal 25-GeV protons in collisions with the nuclei of the aluminum target. A system of quadrupole magnets, bending magnets, and an electromagnetic separator was used to focus, momentum select, and separate the K^- from other particles. The beam transport system is described separately in the Appendix.

The beam was successful from the point of view of intensity. The rate of stopped K^- 's in the chamber was 2 per 5×10^{10} protons on the target. On the other hand, the background in the chamber due to scattering and μ 's from π decay was undesirably large. However, for a stopping K^- experiment, although this background inconvenienced the scanning, it did not lead to misidentification of events. The beam momentum chosen was 700 MeV/c. The K^- were degraded in a carbon absorber immediately before entering the chamber. A typical photograph has about 2 stopping K^- and about 20 extraneous tracks. A photograph with a typical $\Sigma^0 \rightarrow \Lambda^0 + e^+ + e^-$ decay is shown in Fig. 2. The background tracks are readily distinguishable from the stopping K^- because the background tracks are generally minimum ionizing, do not stop, rarely interact, are of higher momentum and are chiefly in a different area of the chamber.

¹⁷ T. Fulton (private communication).

¹⁸ R. Hofstadter, F. Bumiller, and M. R. Yearian, *Rev. Mod. Phys.* **30**, 482 (1958).

B. Analysis

1. Selection of Events

The 400 000 pictures taken in the stopping K^- beam were scanned for events in which the heavily ionizing K^- interacts, two lightly ionizing tracks leave the vertex, and a Λ^0 decay vertex is associated. These events were measured, using standard bubble chamber techniques. The measurements of track coordinates are used as input data for the geometrical reconstruction program NP54.¹⁹ The direction, curvature, and the length of stopping tracks are obtained, as well as the errors in these quantities. The momentum at the midpoint of each track is obtained from the curvature of the track and from the known magnetic field in the chamber. It is, of course, not possible to obtain the momentum of the particle at production until it has been assigned a mass so that the proper range-momentum loss corrections can be made. This is done in the next step in the analysis.

The output of NP54, which does not depend on the masses of the particles in the event, is used as the input to a kinematical fitting program. For this experiment, the program GRIND²⁰ was used. Each event is analyzed by assigning masses to the measured tracks and fitting the event to various kinematical hypotheses. For each hypothesis, GRIND performs an iteration to minimize the chi-square, adjusting the measured quantities in accord with their errors, until a final balance of energy and momentum is achieved with the minimum chi-square.

Each event was fitted to the hypotheses

$$\begin{aligned}
 (1) \quad & K^- + p \rightarrow \Sigma^0 + \pi^0, \\
 & \Sigma^0 \rightarrow \Lambda^0 + e^+ + e^-, \\
 & \Lambda^0 \rightarrow p + \pi^-, \\
 (2) \quad & K^- + p \rightarrow \Lambda^0 + \pi^0, \\
 & \Lambda^0 \rightarrow p + \pi^-, \\
 & \pi^0 \rightarrow \gamma + e^+ + e^-.
 \end{aligned}$$

Of the 1600 events measured, 321 of the events fitted hypotheses (1) with a probability greater than 2%; 199 of the events fitted hypotheses (2) with a probability greater than 2%; 7 of the events fitted both sets of hypotheses with probability greater than 2%.

We estimate the contamination of the sample due to reaction (2) to be about 1%. Consider now, the remaining events which failed to fit either hypotheses (1) or (2).

A few of these events are misidentifications on the

¹⁹ NP54 is a geometrical reconstruction program for bubble chamber tracks, which was written originally by Professor R. Plano and is now maintained by F. Wuensch, Nevis.

²⁰ GRIND is a multivertex kinematical fitting program, written at CERN under the direction of Dr. R. Böck.

part of the mesurer, such as

$$\begin{aligned} K^- + p &\rightarrow \Sigma^+ + \pi^-, \\ \Sigma^+ &\rightarrow p + \pi^0, \\ \pi^0 &\rightarrow e^+ + e^- + \gamma. \end{aligned}$$

These events might be construed by the mesurer to be Σ^0 decays followed immediately by the decay of the Λ^0 . The contamination of our data from this source is negligible.

The rest of the events are either K^- captures with $\Sigma^0 - \pi^0$ production in which the Dalitz pair is produced in π^0 decay:

$$\begin{aligned} (3) \quad K^- + p &\rightarrow \Sigma^0 + \pi^0, \\ \Sigma^0 &\rightarrow \Lambda^0 + \gamma, \\ \pi^0 &\rightarrow \gamma + e^+ + e^-, \end{aligned}$$

or they are events of type (1), (2), or (3) produced by K^- mesons in flight.

Events of type (3) cannot be fitted because they are not overdetermined. The background due to these events has been estimated in two ways. First, random events of this sort were generated by a computer, using the program *mock*.²¹ The *mock*-generated tracks were assigned slightly larger than typical errors, and these events were then fitted to the $\Sigma^0 \rightarrow \Lambda^0 + e^+ + e^-$ decay hypothesis (1), using the kinematical fitting program *GRIND*. Of the *mock*-generated events, 2% fitted hypothesis (1), and since there are twice as many Dalitz pairs from π^0 decay as from Σ^0 decay, it was thought that a maximum of 4% of the events accepted as Σ pair decays might be actually π^0 Dalitz pair decays.

The background due to this source and due to interactions in flight may also be estimated experimentally.

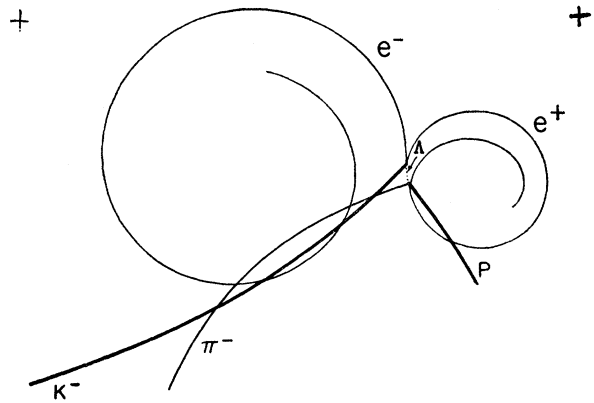
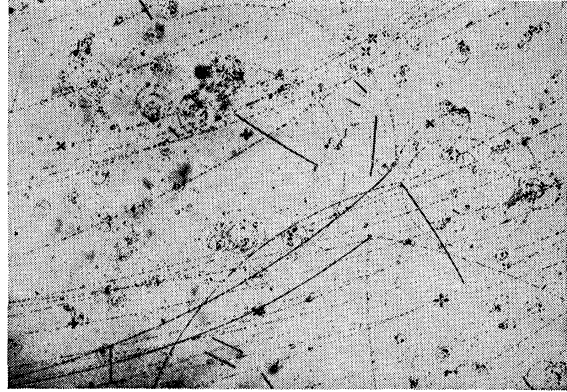


FIG. 2. A chamber photograph with a typical $\Sigma^0 \rightarrow \Lambda^0 + e^+ + e^-$ decay.

In Fig. 3 we have plotted the combined measured mass of the $(\Lambda^0 + e^+ + e^-)$ versus the combined measured momentum of the $(\Lambda^0 + e^+ + e^-)$ for all accepted events. In

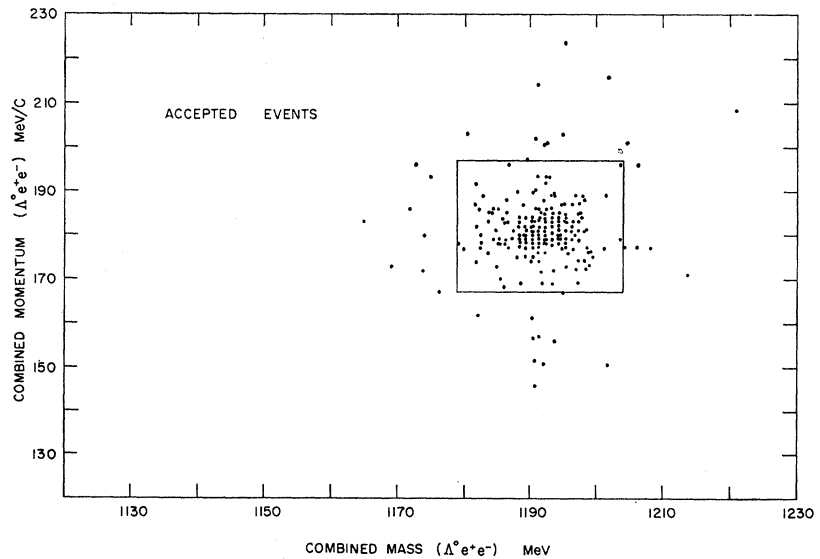


FIG. 3. The combined mass of the $(\Lambda^0 e^+ e^-)$ versus the combined momentum of the $(\Lambda^0 e^+ e^-)$ for events which fitted the criteria for acceptance as $\Sigma^0 \rightarrow \Lambda^0 + e^+ + e^-$.

²¹ *MOCK* is a program written by Professor R. Plano of Rutgers which generates "random" (uncorrelated) numbers and simulates statistically varying data.

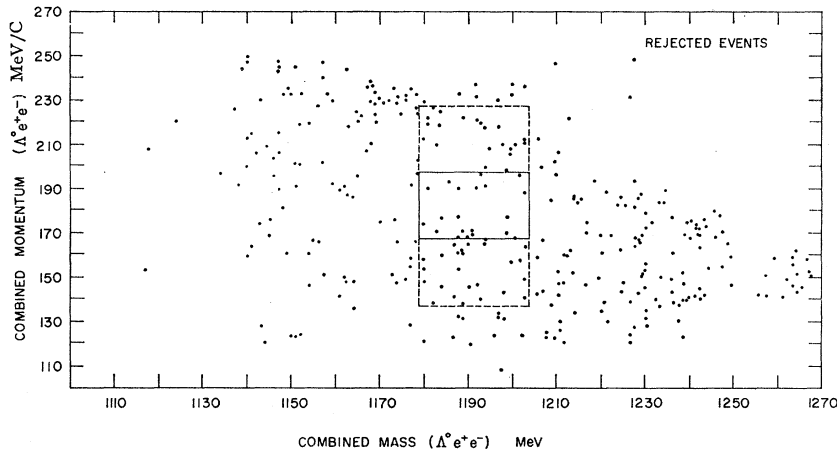


FIG. 4. The combined mass of the $(\Lambda^0 e^+ e^-)$ versus the combined momentum of the $(\Lambda^0 e^+ e^-)$ for events which failed to fit the $\Sigma^0 \rightarrow \Lambda^0 e^+ e^-$ hypothesis.

Fig. 4, we have plotted a similar graph for all rejected events. For the true events, the combined momentum of the $(\Lambda^0 + e^+ + e^-)$ centers about 182 MeV/c, which is the momentum of the Σ^0 produced in the reaction $K^- + p \rightarrow \Sigma^0 + \pi^0$ at rest, and the combined mass of the $(\Lambda^0 + e^+ + e^-)$ centers about 1192.4 MeV, the mass of the Σ^0 . By comparing the density of events which do not fit the $\Sigma^0 \rightarrow \Lambda^0 + e^+ + e^-$ hypothesis, inside and outside the region of acceptance, we find that the density of rejected events is roughly constant, allowing for statistical fluctuations. If a large number of false events had been included in the sample, then rejected events in the region of acceptance would be substantially less than that in the surrounding region. This is not the case, and we take the square root of the number of rejected events in our arbitrary region of acceptance as an upper limit on the number of false events present in our sample. The contamination estimated in this way is 1%.

It should be noted, for the purpose of the analysis

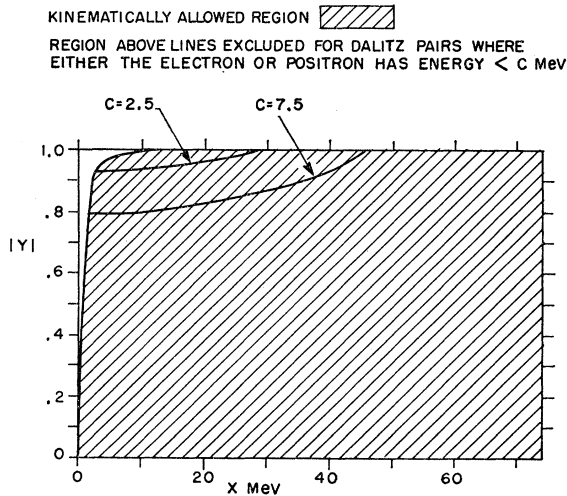


FIG. 5. The region in x and y which is kinematically excluded if low-energy electrons and positrons are not observed, together with the kinematically allowed region.

which follows, that the background events also contain Dalitz pairs, which behave on the whole as the Dalitz pairs from Σ^0 decay, so that a background of the magnitude encountered here has an entirely negligible effect on the conclusions.

A possible source of systematic error in the experiment is due to a scanning bias. If either the electron or positron has a small radius of curvature, the event may be

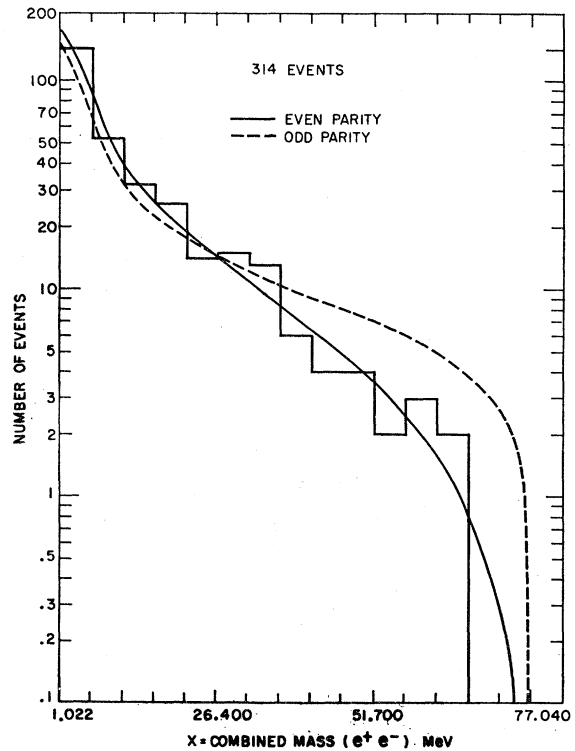


FIG. 6. A histogram of the combined mass spectrum of the Dalitz pair, together with the theoretical spectra for odd and even parity. To facilitate comparison, the theoretical spectra have been integrated over the corresponding histogram intervals and the smoother functions thus obtained are shown.

missed. The magnetic field in the chamber is approximately 14 kg, so that an electron with momentum 3 MeV/c has a radius of curvature of 0.7 cm. The atypical appearance of an event with such an electron may cause it to be missed. However, we may correct for this bias. Let us assume that we will observe no events where either the electron or positron energy is less than C MeV. There is then an additional constraint on the parameters x and y .

$$|y| < \frac{(|\mathbf{P}_+ + \mathbf{P}_-|^2 + x^2)^{1/2} - 2C}{|\mathbf{P}_+ + \mathbf{P}_-|}$$

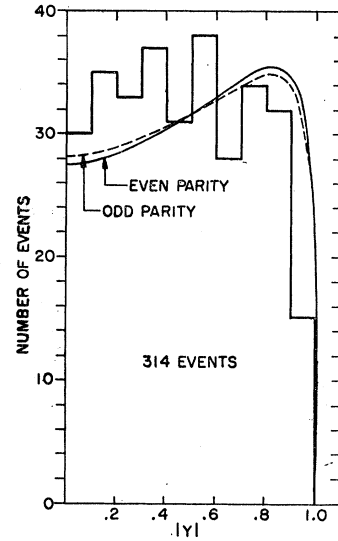
The effect of this kinematical restriction is shown in Fig. 5. We may then avoid this bias by deliberately restricting our selection of experimental events to those where the electron and positron energies are greater than 10 MeV. In the discussion which follows, we have made this restriction on the experimental data and have similarly corrected the theoretical prediction. The experimental distributions in x and y are shown in Figs. 6 and 7, respectively, and the x - y distribution in Fig. 8.

2. Analysis of the Experimental Results

Inspection of Fig. 5 shows that the data are consistent with even parity, but in disagreement with the odd parity predictions for $F_1=0$ and $F_2(x)=F_2(0)$.

The statistical analysis can be refined using the likelihood method. In this way we can test the fit in x and y simultaneously. We no longer make the assumption that F_1 is small, but retain the assumption that both form factors are constant. The likelihood functions are

FIG. 7. A histogram in $|Y|$ of the data together with the theoretically predicted spectra for odd and even parity.



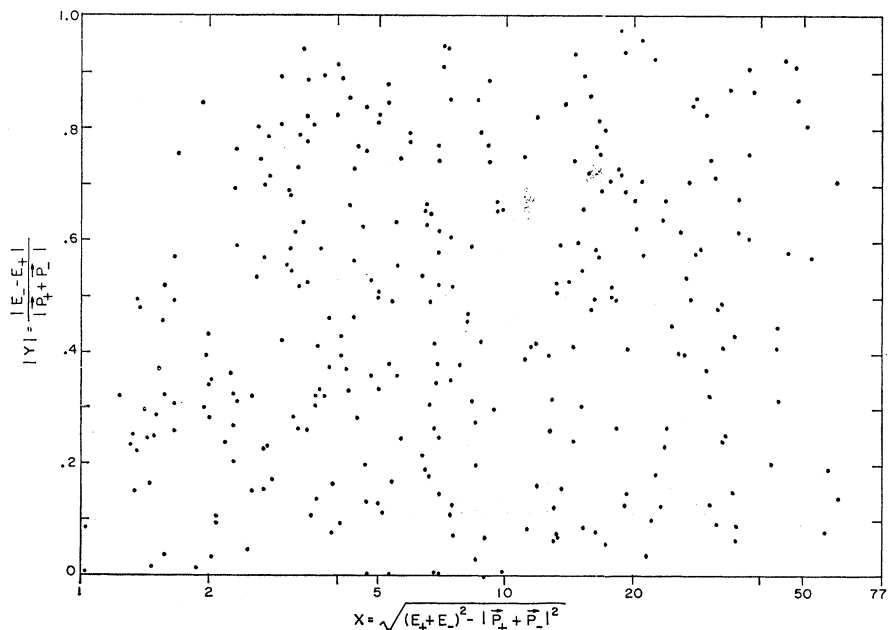
defined to be the products

$$L^\pm = \prod_i \frac{d^2 \rho_\pm(x_i y_i)}{dx dy}$$

where ρ_\pm are the distribution functions of Eq. (1), normalized to 314 events. The logarithms of these functions, being more slowly varying, are the functions actually used in the analysis.

To see that this method of analysis is likely to be fruitful, we calculate the expected likelihood ratio for the case $F_1=0$. Assuming that the parity is even, we expect the experimental distribution to be $d\rho_+(x)/dx$. The expected average logarithm of $d\rho_+(x)/dx$ will

FIG. 8. A scatterplot of the x and y distributions of the data.



then be

$$\int \frac{d\rho_+(x)}{dx} \ln\left(\frac{d\rho_+(x)}{dx}\right) = \left\langle \ln\left(\frac{d\rho_+(x)}{dx}\right) \right\rangle.$$

The expected average logarithm of the odd parity function when the data are actually distributed according to the even function is then

$$\int \frac{d\rho_+(x)}{dx} \ln\left(\frac{d\rho_-(x)}{dx}\right) dx = \left\langle \ln\left(\frac{d\rho_-(x)}{dx}\right) \right\rangle.$$

Thus, if our data consist of N events, the likelihood ratio which we may expect is

$$\exp N \left[\left\langle \ln\left(\frac{d\rho_+(x)}{dx}\right) \right\rangle - \left\langle \ln\left(\frac{d\rho_-(x)}{dx}\right) \right\rangle \right] = e^{N[0.0362]}.$$

The root mean square spread of the logarithm of the likelihood ratio may also be computed.

$$\begin{aligned} \left\langle \left[\ln\left(\frac{d\rho_+(x)/dx}{d\rho_-(x)/dx}\right) - \left\langle \ln\left(\frac{d\rho_+(x)/dx}{d\rho_-(x)/dx}\right) \right\rangle \right]^2 \right\rangle \\ = \left\langle \ln^2\left(\frac{d\rho_+(x)/dx}{d\rho_-(x)/dx}\right) \right\rangle \\ - \left\langle \ln\left(\frac{d\rho_+(x)/dx}{d\rho_-(x)/dx}\right) \right\rangle^2 = (0.22)^2. \end{aligned}$$

One would therefore expect for a sample of N events the root mean square deviation to be $(0.22)\sqrt{N}$.

The result for the 314 unambiguous events reported here is

$$\begin{aligned} \frac{L^+ \prod_i [d\rho_+(x_i)]/dx}{L^- \prod_i [d\rho_-(x_i)]/dx} &= 2.65 \times 10^7, \\ \ln L^+ - \ln L^- &= \sum \ln\left(\frac{d\rho_+(x_i)/dx}{d\rho_-(x_i)/dx}\right) = 13.5. \end{aligned}$$

The root mean square deviation of the logarithm of the likelihood function for 314 events is 3.9. This result is therefore strongly in favor of even parity.

We now consider the possibility that $F_1 \neq 0$. The F_1 terms of the even parity distribution have, in addition to the factor x^2/M^2 , the small factor $M_\Sigma - M_\Lambda$, so that the F_1 term here can be neglected.

The odd parity distribution depends more strongly on F_1/F_2 , and becomes very similar to the even parity distribution at $F_1/F_2 \cong 8$. To show the dependence of the distributions on F_1/F_2 , we have minimized the integral

$$\int \left[\frac{d\rho_+(x)}{dx} - \frac{d\rho_-(x)}{dx} \right]^2 dx$$

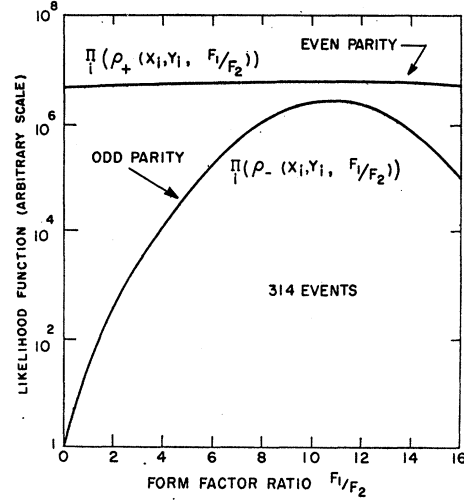


FIG. 9. Likelihood of the data for even and odd parity as a function of F_1/F_2 .

with respect to the parameter F_1/F_2 . For $F_1/F_2 \sim 8.5$, the even and odd parity distributions are very nearly the same.

The likelihood as a function of F_1 has also been calculated, assuming that F_1 and F_2 are independent of x . The result is shown in Fig. 9. The greater sensitivity to F_1/F_2 of the odd spectrum is reflected in the behavior of the likelihood functions, the odd parity likelihood varying sharply with F_1/F_2 while the even parity likelihood function remains flat. For a small range of values near $F_1/F_2 \sim 11$ the odd parity likelihood is comparable to the even parity likelihood.

These results imply even Σ - Λ relative parity. There are two points to be made in reaching this conclusion. The first point is that the data in any case fit the predictions based on even parity independent of form factor assumptions, but are not compatible with the predictions based on odd parity in the range of values for

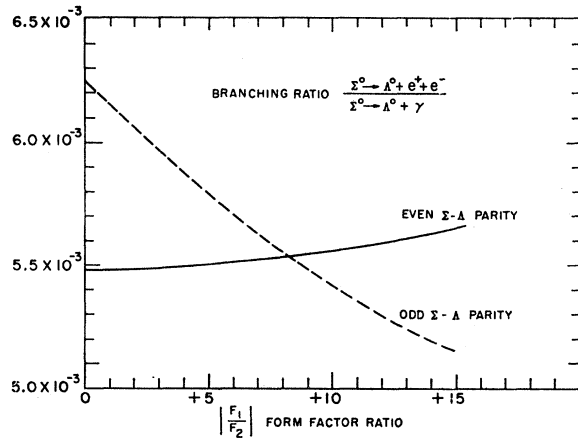


FIG. 10. The branching ratio $(\Sigma^0 \rightarrow \Lambda^0 + e^- + e^+)/(\Sigma^0 \rightarrow \Lambda^0 + \gamma)$ versus F_1/F_2 .

the form factor F_1 which seems likely on theoretical grounds (see the discussion of Sec. II).

The second point is the following: If the theoretical suggestions on the magnitude of F_1 are not granted and all values of F_1 are considered possible, the data can indeed be fitted with the odd parity, taking $F_1 = 11 \pm 3$.

It would then be a remarkable coincidence for the $\Sigma - \Lambda$ parity to be odd, and for the odd parity spectrum, which varies substantially with F_1/F_2 to simulate the even parity spectrum, which is almost independent of F_1/F_2 . The similarity of the even parity distribution and the odd parity distribution with $F = 8.5$ is very close. It would take a large increase (perhaps a hundredfold) in statistical accuracy to resolve the two.

It is clear from Fig. 10 that a measurement of the branching ratio

$$R = \frac{\Sigma^0 \rightarrow \Lambda^0 + e^+ + e^-}{\Sigma^0 \rightarrow \Lambda^0 + \gamma}$$

would not resolve the ambiguity since for $F_1/F_2 \approx 8.5$ the two parities give the same rate.

Our result confirms that of Courant *et al.*²² who have studied the same decay.

ACKNOWLEDGMENTS

We are very grateful for the assistance and cooperation of G. K. Green, M. H. Blewett, H. N. Brown, and the staff of the AGS. We also wish to thank the crew of 30-in. Brookhaven National Laboratory-Columbia Hydrogen Bubble Chamber for maintaining and operating the chamber during the run.

APPENDIX I

Separated Low-Momentum Beam

In order to obtain stopping K^- mesons in the hydrogen bubble chamber, a separated low momentum K^-

beam was installed at the AGS. The beam is designed to operate over a range of momenta from 500 to 900 MeV/c, the lower and upper limits being determined by excessive decay attenuation and insufficient separation, respectively.

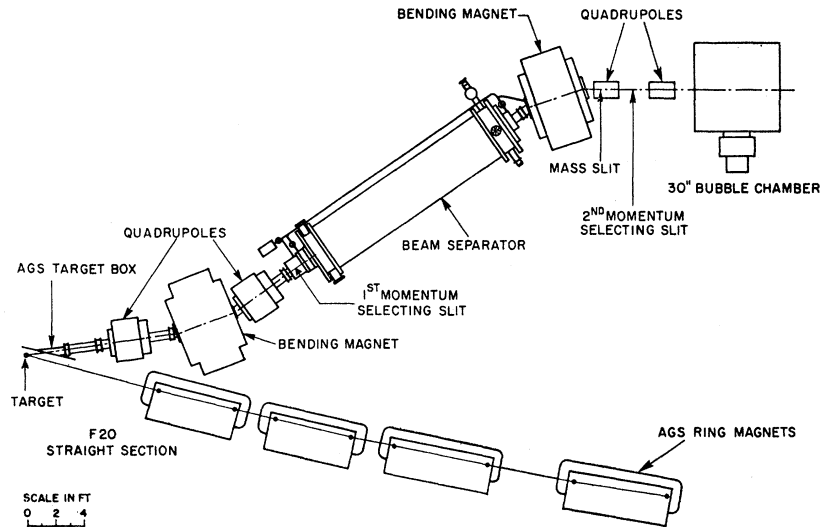
Figure 11 shows a layout of the beam. The beam is extracted at an angle of 23° with respect to the circulating protons. There is a single stage of separation. There are three irises, two vertical slits for momentum analysis, and one horizontal slit for velocity analysis. The electrodes are 5 m long. An electric field of 45 kV/cm is maintained between the electrodes. The first and second bending magnets deflect 26° and 36° , respectively. Typical particle trajectories, without the bending, are shown in Figs. 12 and 13. The first, third and fourth quadrupoles focus in a horizontal plane, the second quadrupole focuses vertically. The fourth quadrupole is used to shape the beam for efficient use of the bubble chamber.

The particles are transported in vacuum from the target to the third quadrupole. Mylar windows separate the machine vacuum, beam vacuum, and separator vacuum. The thicknesses of these windows were 1 mil at the AGS beamport, 0.1 mil at either end of the separator, and 10 mils at the end of the vacuum just before the vertical focus.

Separated Low-Momentum K^- Beam Parameters

Length from target to bubble chamber	18 in.
Target area	0.25×0.25 in. \perp to beam
Solid angle	0.6 msr
Momentum bite	$\pm 1\%$

FIG. 11. A layout of the separated K^- beam.



²² H. Courant, H. Filthuth, P. Franzini, R. G. Glasser, A. Minguzzi-Ranzi *et al.*, Phys. Rev. Letters 10, 409 (1963).

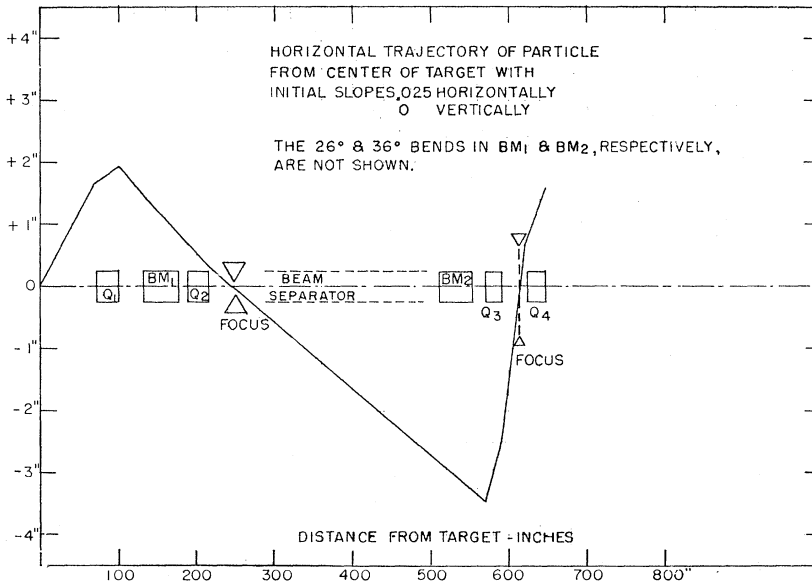


FIG. 12. Beam trajectory projection in the horizontal plane.

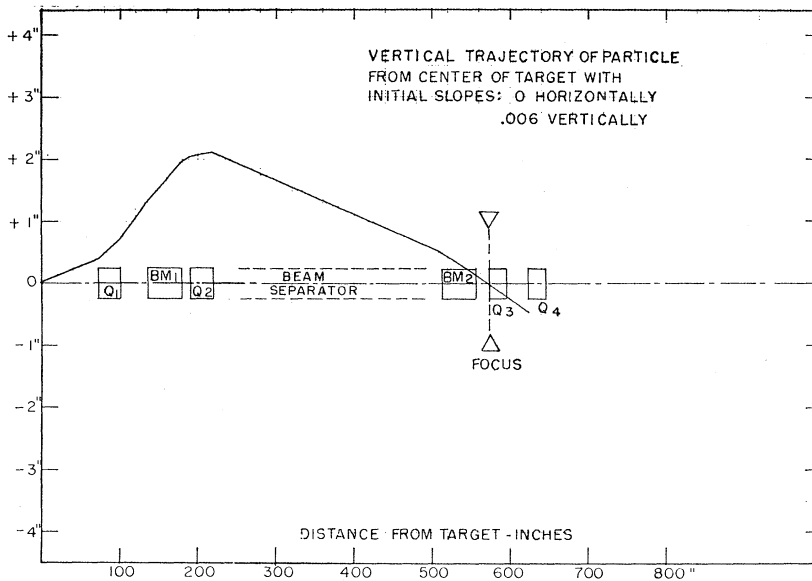


FIG. 13. Beam trajectory projection in the vertical plane.

First horizontal focus:

Magnification 2.3
Image size 0.57 in.
Momentum dispersion at 600 MeV/c 0.08 in./MeV/c
Slit width 1.1 in.

Second horizontal focus:

Magnification 0.24
Image size 0.06 in.
Momentum dispersion at 600 MeV/c 0.035 in./MeV/c
Slit width 0.6 in.

Vertical focus:

Magnification 0.74
Slit height 0.25 in.

The separation in general is in inches.

$$\frac{E(V/cm)5.45 \times 10^4}{(1/\beta_\pi - 1/\beta_K) pc(eV)}$$

Intensity 2 K⁻ stopping/5 × 10¹⁰ protons on target.

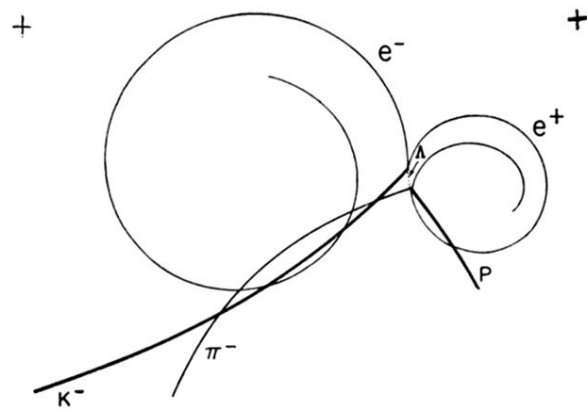
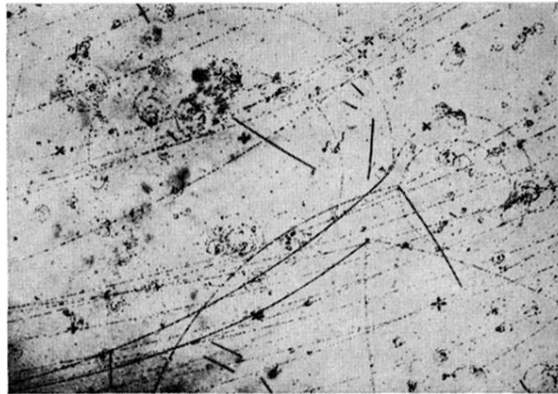


FIG. 2. A chamber photograph with a typical $\Sigma^0 \rightarrow \Lambda^0 + e^+ + e^-$ decay.